Biogeosciences Discuss., 9, 1055–1096, 2012
www.biogeosciences-discuss.net/9/1055/2012/
doi:10.5194/bgd-9-1055-2012

Biogeosciences
Discussions

Differential long-term effects of climate change and management on stocks and distribution of soil organic carbon in productive grasslands

A. M. G. De Bruijn[1,2], **P. Calanca**[1], **C. Ammann**[1], **and J. Fuhrer**[1]

[1] Agroscope ART, Federal Research Station, Air pollution/Climate Group,
Reckenholzstrasse 191, 8046 Zürich, Switzerland
[2] Department of Forestry and Natural Resources, Purdue University,
West Lafayette, IN 47907-2061, USA

Received: 14 October 2011 – Accepted: 12 January 2012 – Published: 24 January 2012

Correspondence to: A. M. G. De Bruijn (adebruij@purdue.edu)

Published by Copernicus Publications on behalf of the European Geosciences Union.

Abstract

We studied the impact of climate change on the dynamics of soil organic carbon (SOC) stocks in productive grassland systems undergoing two types of management, an intensive type with frequent harvests and fertilizer applications and an extensive system where fertilization is omitted and harvests are fewer. The Oensingen Grassland Model was explicitly developed for this study. It was calibrated using measurements taken in a recently established permanent sward in Central Switzerland, and run to simulate SOC dynamics over 2001–2100 under three climate change scenarios assuming different elements of IPCC A2 emission scenarios. We found that: (1) management intensity dominates SOC until approximately 20 yr after grassland establishment. Differences in SOC between climate scenarios become significant after 20 yr and climate effects dominate SOC dynamics from approximately 50 yr after establishment, (2) carbon supplied through manure contributes about 60 % to measured organic C increase in fertilized grassland. (3) Soil C accumulates particularly in the top 10 cm soil until 5 yr after establishment. In the long-term, C accumulation takes place in the top 15 cm of the soil profile, while C content decreases below this depth. The transitional depth between gains and losses of C mainly depends on the vertical distribution of root senescence and root biomass. We discuss the importance of previous land use on carbon sequestration potentials that are much lower at the Oensingen site under ley-arable rotation and with much higher SOC stocks than most soils under arable crops. We further discuss the importance of biomass senescence rates, because C balance estimations indicate that these may differ considerably between the two management systems.

1 Introduction

Grasslands tend to store more carbon (C) than arable lands, most C in the soil being organic (Soil Organic Carbon). For this reason, previous studies have focused on land use conversion as a measure to mitigate climate change (Schimel, 1995; IPCC, 2000; Conant et al., 2001; Ammann et al., 2007; Lal, 2007; Poeplau et al., 2011). Some published estimates based on measured changes in SOC (ΔSOC) in new grasslands are shown in Table 1. Discussion has evolved however, on the importance of management on SOC in grassland (Ammann et al., 2007; Leifeld and Fuhrer, 2010; van Wesemael et al., 2010).

Dynamics of SOC tend to be mainly driven by litter input and soil respiration, but additional import of manure-derived C has also been shown to increment SOC substantially (Leifeld and Fuhrer, 2010; Van Wesemael et al., 2010). Ammann et al. (2007) found that ΔSOC is negative in a newly established grassland when it is not fertilized. Furthermore, effects of climate changes on the efficiency of grassland establishment as a mitigation policy are uncertain (Kätterer, 1998; IPCC, 2000; De Bruijn and Butterbach-Bahl, 2010). Some climatic drivers (air temperature and precipitation) effect both C input by vegetation growth and soil respiration, while others (radiation, atmospheric CO_2 concentrations) effect growth alone. Further consideration deserves also ΔSOC in deeper soil. Estimates of total SOC, for example by IPCC (2000) or Poeplau et al. (2011) are typically based on statistical upscaling of field measurements. Field sampling however, tends to focus in the upper soil (~30 cm) whereas 70 % of SOC is typically located below 20 cm depth (Poeplau et al., 2011).

The goal of our study was to examine how ΔSOC depends on climate and management at different soil depths and time scales in a newly established grassland. Biogeochemical models have proven useful to improve knowledge about long-term ΔSOC (DNDC: Li et al., 1992, RothC: Jenkinson, 1991, PaSim: Riedo et al., 1998, Century: Parton et al., 1987; Kulshreshtha and Sobool, 2006). An issue which has been identified in some of the commonly used biogeochemical models is a loss of robustness, model stiffness or over-parameterization, due to the complexity of dealing with a large range of biological, chemical and physical processes (Kesik et al., 2005; De Bruijn and Butterbach-Bahl, 2010).

We developed a new semi-empirical computer simulation model that describes interactions between plant and soil C:N processes to study ΔSOC after conversion of cropland to grassland at a site in Central Switzerland (Oensingen). The Oensingen Grassland Model (OGM) was calibrated using measurements taken in 2002–2009 at the ongoing long-term experiment at Oensingen that started in 2000. These data are particularly valuable because two parallel plots were established on the same arable field, but developed under different management (Ammann et al., 2007, 2009). Model runs were used to simulate long term (100 yr) ΔSOC under variable management and climatic conditions.

2 Materials and methods

2.1 Field observation dataset

Relevant measurements are shown in Table 2. The FLUXNET grassland site Oensingen is located in central Switzerland (7°44′ E, 47°17′ N, 450 m a.s.l.). It has a mixed maritime/continental climate with high annual rainfall (1100 mm). Mean annual air temperature is 9.5 °C. The soil is classified as Eutri-Stagnic Cambisol (FAO, ISRIC and ISSS, 1998) developed on clayey alluvial deposits. Clay content is between 42 and 44 %, total pore volume is 50–55 % and fine pore volume is 32 %. Before 2000, the field has been under ley-arable rotation with a typical 8-yr cycle. Fertilization with N depended on crop type and followed the Swiss standard fertilization practice (110 kg N ha^{-1} yr^{-1} on average). The field was last ploughed in November 2000 after which it was divided into two equal sized (0.77 ha) rectangular plots (Ammann et al., 2007).

The two management systems were named intensive management (INT) and extensive management (EXT) in previous publications that discuss the Oensingen experiments (Ammann et al., 2007, 2009; Leifeld et al., 2010). The plots were sown in May 2001: INT with 7 species of grass and clover, EXT with 30 species of grass, clover and herbs (Ammann et al., 2009). Grass clippings are usually hayed except for the last cut, which is fermented. INT is fertilized with solid ammonium nitrate (±120 kg ha^{-1} per treatment) or liquid cattle manure (±32 $\text{m}^3\,\text{ha}^{-1}$ per treatment) at the beginning of each growing cycle. EXT remains unfertilized. The number of harvests depended on the observed productivity of the field and followed the normal agricultural practice in the region. EXT typically remained uncut until June and is typically cut 3 times per year whereas INT is typically cut 4 times per year. Ammann et al. (2009) found that EXT had a negative N balance during 2001–2006.

2.2 Model description

In general, we were aiming to maintain the advantages of a process-based model (e.g. the ability to improve qualitative understanding rather than just to quantify relevant processes), while using few parameters and mathematical descriptions that are basic. The OGM model simplifies by lumping molecular varieties in which C and N elements occur in the soil and vegetation, it does not explicitly calculate microbial population dynamics, uses few decomposition pools and a limited number of input parameters. When compared to some of the more frequently used biogeochemical models, it resembles RothC and Century rather than DNDC or PaSim. In contrast with RothC and Century however, it maintains daily integration steps rather than monthly or annual. The development of a new model, moreover, allowed us to experiment with some alternative approaches.

OGM simulates a soil-plant system in one spatial dimension, with modules for temperature, moisture and C and N dynamics (Fig. 1). It uses three driving climatic variables (temperature, radiation, and precipitation), atmospheric CO_2 concentration, 4 input parameters per soil layer (bulk density, porosity, C content and C:N ratio), 19 parameters that are specific for a vegetation type (e.g. water use efficiency, root/shoot turnover rate, Specific Leaf Area), and 24 parameters that are site or soil type specific (e.g. potential decomposition rates, optimum decomposition temperature, moisture). The latter, when describing soil properties, are assumed constant with soil depth. The

OGM model uses a daily time step, with daily averages for temperature and radiation, and daily sums for precipitation. The user can decrease the time step to prevent oscillations. Results presented here were obtained with an hourly time step. The model integrates virtual soil layers, assuming constant conditions in each layer. The user can set the thickness of each layer depending on research interests and the availability of data. For the present simulations, the soil profile was divided into 11 layers (2 × 5 cm, 9 × 10 cm) to simulate down to 1.0 m depth. OGM has a Microsoft windows-specific (Visual C++) user interface which is separated from the model calculations that are ansii compliant (C++).

2.2.1 Temperature and moisture

The temperature submodel is common to many soil biogeochemistry models; we will not describe it in detail here. A simple cascade approach was used to model soil moisture. The main processes that drive soil moisture are soil water movement and uptake of soil moisture by the vegetation. Water movement depends on water potentials that change with soil moisture in adjacent layers. Water uptake depends on soil moisture and root density. Further details of the water and temperature submodel can be found in Müller (2000).

2.2.2 Carbon and nitrogen balance

Plants can assimilate atmospheric CO_2 and fix N_2 through root symbiosis with rhizobia (Biological Nitrogen Fixation, BNF). The model treats organic manure-related additions of C and N (organic manure is always cattle slurry in INT) similar to inputs of plant residues since it increases the decomposition pools according to concentrations of C, N and a fraction of manure that is labile.

While acknowledging that there is ongoing discussion about the biophysical interpretation of modeled decomposition pools, OGM confirms with models such as RothC, DNDC, COUP or also the century model, by using conceptual rather than measurable decomposition pools, mainly in order to reduce the number of pools and to simplify model parameterization (De Bruijn and Butterback-Bahl, 2010; Parton et al., 1987; Li et al., 1992; Xu et al., 2011). OGM uses four decomposition pools, two for C and two for N distinguished according to decomposability (C_{labile} N_{labile}, $C_{\text{recalcitrant}}$, $N_{\text{recalcitrant}}$). Inorganic manure-bound N increases a separate pool of dissolved N, which represents both organic (DON) and inorganic (DIN) nitrogen ($N_{\text{diss}_{\text{sl}}}$: DON+DIN in soil layer sl). Extraction of C and N occurs with harvests, net emission of CO_2 and nitrogenous gases, or through leaching of $N_{\text{diss}_{\text{sl}}}$. Leaching of DOC has not been investigated at the Oensingen field site, but Zeeman (2008) found that C leaching in a similar site in Switzerland was very small ($0.05\,\text{t}\,\text{C}\,\text{ha}^{-1}\,\text{yr}^{-1}$).

OGM calculates gaseous N emissions ($N_{\text{emissions}}$) or N leachates (N_{leaching}), but it does not specify species of N gases (N_xO_y, NH_3^+) or leachates (DON, NO_3^-, NH_4^+). In consequence, OGM cannot be calibrated for accuracy of N emission rates, even though emissions are constrained by the decomposition rates and C:N ratio of the decomposition pools in the model. The OGM model uses plant functional types (i.e. categories of species with similar biochemical characteristics) to deal with interspecies variability. Biochemical behavior of a functional type is described with unified equations that can be parameterized differently. For the present simulations two plant functional types were used: legumes ($v = 0$) and grasses ($v = 1$). In the following, subscripts "v", "d" and "sl" are used to refer to individual vegetation types $\{v = 0,1$ for grass and legumes$\}$, decomposition pools $\{d = 0,1$ for labile and recalcitrant$\}$, and soil layers $\{\text{sl} = 0$, slMax for increasing depth$\}$.

Net ecosystem exchange (NEE) is the sum of CO_2 assimilation and respiration:

$$\text{NEE} = \sum_{v=0}^{1} \left(\frac{\delta C}{\delta t}\right)_{\text{assim},v} - \sum_{d=0}^{1} \left(\frac{\delta C}{\delta t}\right)_{\text{decomposition},d} \tag{1}$$

where $(\frac{\delta C}{\delta t})_{\text{assim},v}$ is net assimilation by v, and $(\frac{\delta C}{\delta t})_{\text{decomposition},d}$ is decomposition-related loss of C from d. Net biomass productivity (NBP) is the sum of C input and losses including management induced changes:

$$\mathrm{NBP}=\mathrm{NEE}+\left(\frac{\delta \mathrm{C}}{\delta t}\right)_{\mathrm{manure}}-\sum_{v=0}^{1}\left(\frac{\delta \mathrm{C}}{\delta t}\right)_{\mathrm{harvest,v}} \tag{2}$$

where $(\frac{\delta \mathrm{C}}{\delta t})_{\mathrm{harvest,v}}$ is biomass that is removed with harvests and $(\frac{\delta \mathrm{C}}{\delta t})_{\mathrm{manure}}$ is manure-bound C. All variables are expressed in $\mathrm{g\,C\,m^{-2}}$. The N balance is calculated according to:

$$\left(\frac{\delta \mathrm{N}}{\delta t}\right)_{\mathrm{system}}=\sum_{v=0}^{1}\left(\left(\frac{\delta \mathrm{N}}{\delta t}\right)_{\mathrm{BNF,v}}-\left(\frac{\delta \mathrm{N}}{\delta t}\right)_{\mathrm{harvest,v}}\right)+\left(\frac{\delta \mathrm{N}}{\delta t}\right)_{\mathrm{manure}}-\left(\frac{\delta \mathrm{N}}{\delta t}\right)_{\mathrm{emission}}-\left(\frac{\delta \mathrm{N}}{\delta t}\right)_{\mathrm{leaching}} \tag{3}$$

where $(\frac{\delta \mathrm{N}}{\delta t})_{\mathrm{BNF,v}}$ is N fixation by v, $(\frac{\delta \mathrm{N}}{\delta t})_{\mathrm{harvest,v}}$ is N that is removed with harvest. $(\frac{\delta \mathrm{N}}{\delta t})_{\mathrm{manure}}$ is manure-bound N, $(\frac{\delta \mathrm{N}}{\delta t})_{\mathrm{emission}}$ is N gaseous emission. $(\frac{\delta \mathrm{N}}{\delta t})_{\mathrm{leaching}}$ is N leaching. All variables are expressed in $\mathrm{g\,N\,m^{-2}}$.

2.2.3 Vegetation

Steduto et al. (2009) developed the AquaCrop model which assumes that plant growth correlates well with crop transpiration under nutrient-saturated conditions. In agreement with AquaCrop, OGM uses crop transpiration as the main driver of assimilation:

$$\left(\frac{\delta \mathrm{C}}{\delta t}\right)_{\mathrm{assim,v}}=\mathrm{Ns_v}\cdot\mathrm{WUE_v}\cdot\left(1.0+P_{\mathrm{CO_2,v}}\right)\cdot\mathrm{Tr_v} \tag{4}$$

where $\mathrm{WUE_v}$ is the potential water use efficiency of v under pre-industrial levels of atmospheric $\mathrm{CO_2}$ ($\mathrm{g\,C\,mm^{-1}\,H_2O}$), $\mathrm{Ns_v}$ is a growth rate reduction factor that depends on the concentration of N in leaves and $\mathrm{Tr_v}$ is transpiration by v. $P_{\mathrm{CO_2}}$ is the relative increase of WUE (%) with increasing concentrations of atmospheric $\mathrm{CO_2}$:

$$P_{\mathrm{CO_2,v}}=\frac{D_{\mathrm{CO_2,v}}}{100\,\%}\cdot\left(\frac{\rho_{\mathrm{CO_2}}-370}{370}\right) \tag{5}$$

where ρ_{CO_2} is the concentration of atmospheric CO_2 in ppm, $D_{CO_2,v}$ is the rate increase of photosynthesis in v if atmospheric concentration of CO_2 doubles compared to pre-industrial $\rho_{CO_2} = 370$ ppm. Published estimates of $D_{CO_2,v}$ for species in INT and EXT range from 20–40 % and estimates of individual species typically differ as much as those between species (Aeschlimann et al., 2005; Ainsworth et al., 2003; Casella and Soussana, 1997; Ryle et al., 1992). In the present model applications, we used $D_{CO_2} =$ 33 % for both grasses and legumes (C3 plants) based on an extensive literature review by Wand et al. (1999).

The N stress factor $\mathrm{Ns_v}$ is calculated from foliage N according to

$$\mathrm{Ns_v} = \left(\frac{\mathrm{C2Nf_v}}{\mathrm{C2N_{OPT,v}}}\right)^{\lambda \mathrm{Ns_v}} \tag{6}$$

where $\mathrm{C2Nf_v}$ and $\mathrm{C2N_{OPT,v}}$ are current and optimal C:N ratio in foliage of v, $\lambda\mathrm{Ns_v}$ is a tuning parameter applied to v, and transpiration $\mathrm{Tr_v}$ is calculated from potential evapotranspiration ($\mathrm{ET_0}$), which is estimated from air temperature and radiation according to Priestley and Taylor (1972). Soil evaporation E and potential transpiration $\mathrm{PT_{tot}}$ ($\mathrm{PT_{tot}} = \Sigma \mathrm{PT_v}$) are calculated from $\mathrm{ET_0}$ using the total leaf area $\mathrm{LAI_{tot}}$ ($\mathrm{LAI_{tot}} = \Sigma \mathrm{LAI_v}$) assuming that E is negligible when $\mathrm{LAI_{tot}} > 1.0\,\mathrm{m^2\,m^{-2}}$ ($\mathrm{PT_{tot}} = \Sigma(\mathrm{LAI_v}\ \mathrm{ET_0})$ when $\mathrm{LAI_{tot}} < 1.0$ or $\mathrm{PT_{SUM}} = \mathrm{ET_0}$ when $\mathrm{LAI_{tot}} > 1.0$). $\mathrm{PT_v}$ is derived from $\mathrm{PT_{tot}}$ using the dominance in foliage cover $\mathrm{dom_v}$ ($\mathrm{dom_v} = \mathrm{LAI_v}/\mathrm{LAI_{tot}}$) assuming that the capacity of a vegetation type to dominate water uptake of an ecosystem with more than one type of vegetation ($\mathrm{PT_v}/\mathrm{PT_{tot}}$) correlates linearly with $\mathrm{dom_v}$ ($\mathrm{PT_v} = \mathrm{dom_v}\ \mathrm{PT_{tot}}$). The actual transpiration of v ($\mathrm{Tr_v}$) is estimated from $\mathrm{PT_v}$ according to root biomass and moisture availability in individual soil layers:

$$\mathrm{Tr_v} = \sum_{\mathrm{sl}=0}^{\mathrm{slMax}} \left(\mathrm{fr_{sl,v}} \cdot \left(\frac{\theta_{\mathrm{sl}} - \theta_{\mathrm{wilt,v}}}{\theta_{\mathrm{poro}} - \theta_{\mathrm{wilt,v}}} \right)^{\lambda s_{\mathrm{v}}} \cdot \mathrm{PT_v} \right) \tag{7}$$

where $\mathrm{fr_{sl,v}}$ is the fraction of root biomass of v in soil layer sl (see also Eq. 12), slMax is the number of soil layers and θ_{sl} is the water content in sl (VOL%), $\theta_{\mathrm{wilt,v}}$ is soil moisture content at the level where v starts to wilt (VOL%), θ_{poro} is water content at field capacity (VOL%) and λs_v is a tuning parameter applied to v. N uptake by plant roots is calculated according to:

$$\left(\frac{\delta \mathrm{N}}{\delta t}\right)_{\text{uptake},\mathrm{v}} = \sum_{\mathrm{sl}=0}^{\mathrm{slMax}} \mathrm{Nup}_{\mathrm{v}} \cdot \mathrm{N}_{\mathrm{diss}_{\mathrm{sl}}} \cdot \mathrm{fr}_{\mathrm{sl,v}} \cdot \mathrm{Br}_{\mathrm{v}} \tag{8}$$

where $\mathrm{Nup}_{\mathrm{v}}$ is uptake capacity by roots of v ($g_{\mathrm{N}}/g_{\mathrm{DW(root)}}$), Br_{v} = root biomass of v ($g_{\mathrm{DW}}\,\mathrm{m}^{-2}$). The OGM model assumes that BNF correlates linearly with root volume:

$$\left(\frac{\delta \mathrm{N}}{\delta t}\right)_{\mathrm{BNF,v}} = \sum_{\mathrm{sl}=0}^{\mathrm{slMax}} \left(\mathrm{BNFC}_{\mathrm{v}} \cdot \mathrm{fr}_{\mathrm{sl,v}} \cdot \mathrm{Br}_{\mathrm{v}}\right) \tag{9}$$

where $\mathrm{BNFC}_{\mathrm{v}}$ is the rate of N_2 fixation by roots of v ($g_{\mathrm{N}}\ g^{-1}_{\mathrm{DW(root)}}$), with $\mathrm{BNFC}_{\mathrm{v}} = 0.0$ when simulating species that are incapable of fixing atmospheric N_2.

Two pools are used to describe vegetation development (Bs: shoot biomass and Br: root biomass; both in $\mathrm{g\,DW\,m^{-2}}$). The density of C in a component is a fixed parameter but the C:N ratio fluctuates. We are assuming that plants improve access to N by investing in roots when the C:N ratio in foliage increases, or vice versa, plants increase foliage biomass to improve assimilation of C when the C:N ratio drops (Thornley and Johnson, 1990):

$$f\mathrm{Ca}_{\mathrm{v}} = \lambda \mathrm{Ca}_{\mathrm{v}} \cdot \left(\frac{\mathrm{C2N}_{\mathrm{OPT,v}}}{\mathrm{C2Ns}}\right) \tag{10}$$

where $f\mathrm{Ca}_{\mathrm{v}}$ is the fraction of assimilated C that is allocated aboveground, $\mathrm{C2N}_{\mathrm{opt,v}}/\mathrm{C2Ns}$ is shoot N status (capped to exclude values larger than 1.0) and $\lambda\mathrm{Ca}_{\mathrm{v}}$ is a tuning parameter applied to v. We further assume that foliage growth and N allocation does not depend on root C:N ratio, and that aboveground allocation of N (fNa: the fraction of N that is allocated to aboveground parts) decreases as C2Ns drops below $\mathrm{C2N}_{\mathrm{opt,v}}$ and roots are used to store excess N.

$$f\mathrm{Na}_\mathrm{v} = 1.0 - \lambda\mathrm{Cb}_\mathrm{v} \cdot \left(\frac{\mathrm{C2N}_{\mathrm{OPT,v}}}{\mathrm{C2Ns}}\right) \tag{11}$$

Root biomass distribution is commonly modeled assuming an exponential decrease of root biomass with depth (Gerwitz and Page, 1974). However, data for root biomass measured at Oensingen suggest that this assumption tends to underestimate root biomass in the top soil layer. Alternatively, we used:

$$\mathrm{Br}_{\mathrm{v,sl}} = \mathrm{Br}_\mathrm{v} \cdot \frac{\left(D_{\mathrm{max}_\mathrm{v}}/D_{\mathrm{sl}}\right)^{\lambda\mathrm{Br}}}{\sum\limits_{\mathrm{sl}=0}^{\mathrm{slMax}} \left(D_{\mathrm{max}_\mathrm{v}}/D_{\mathrm{sl}}\right)^{\lambda\mathrm{Br}}} \tag{12}$$

where $\mathrm{Br}_{\mathrm{v,sl}}$ is root biomass of v in sl, Br_v is the total root biomass of v ($\mathrm{g_{DW}\,m^{-2}}$), $D_{\mathrm{max}_\mathrm{v}}$ is rooting depth of vegetation type v (m), and D_{sl} is the depth of sl (m). Parameter $\lambda\mathrm{Br}$ is a shape parameter. Foliage turnover $(\frac{\delta\mathrm{Bs}}{\delta t})_{\mathrm{turnover,v}}$ depends on an intrinsic turnover rate which expresses the effect of ageing, and of water stress:

$$\left(\frac{\delta\mathrm{Bs}}{\delta t}\right)_{\mathrm{turnover,v}} = \left(\mathrm{TOf}_\mathrm{v} + \lambda\mathrm{sTO}_\mathrm{v} \cdot \frac{\mathrm{TR}_\mathrm{v}}{\mathrm{PT}_\mathrm{v}}\right) \cdot \mathrm{Bs}_\mathrm{v} \tag{13}$$

where TOf_v is reference foliage turnover rate and $\lambda\mathrm{sTO}_\mathrm{v}$ is a shape parameter that increases foliage decay with water stress (m^{-1}). Root biomass turnover $(\frac{\delta\mathrm{Br}}{\delta t})_{\mathrm{turnover,v}}$ is a constant fraction ($\mathrm{TOr}_{\mathrm{rv}}$ in $\mathrm{kg_{DW}\,kg_{DW}^{-1}}$) of root biomass:

$$\left(\frac{\delta\mathrm{Br}}{\delta t}\right)_{\mathrm{turnover,v,sl}} = \mathrm{TOr}_\mathrm{v} \cdot \mathrm{Br}_{\mathrm{v,sl}} \tag{14}$$

The model assumes that harvest index (HI: extracted biomass/cut biomass) is constant regardless of harvesting method:

$$\left(\frac{\delta \mathrm{Bs}}{\delta t}\right)_{\mathrm{harvest,v}} = \mathrm{HI}\cdot\left(\frac{\delta \mathrm{Bs}}{\delta t}\right)_{\mathrm{cut,v}} \tag{15}$$

The volume of cut biomass is estimated by subtracting the aboveground biomass that remains after a cut ($\mathrm{Bi_v}$ is derived from a vegetation specific parameter $\mathrm{LAI_{init,v}}$ that is the LAI of *v* immediately after emergence) from biomass volume at the time of the cut ($\mathrm{Bs_v}$):

$$\left(\frac{\delta \mathrm{Bs}}{\delta t}\right)_{\mathrm{cut,v}} = (1.0-\mathrm{Bi_v})\cdot\mathrm{Bs_v} \tag{16}$$

The remaining biomass (cut but not removed) is added to the soil together with other residues:

$$\left(\frac{\delta \mathrm{C}}{\delta t}\right)_{\mathrm{harv\_litter,v}} = \left(\frac{\delta \mathrm{Bs}}{\delta t}\right)_{\mathrm{cut,v}} - \left(\frac{\delta \mathrm{Bs}}{\delta t}\right)_{\mathrm{harvest,v}} \tag{17}$$

where $(\frac{\delta \mathrm{C}}{\delta t})_{\mathrm{harv\_litter,v}}$ are biomass residues after a harvest.

The current model structure cannot deal with grazing, which is not part of management systems applied at the Oensingen grasslands. Inclusion of grazing would require additional parameterization of cattle density and activity. We do expect however, that model performance in such setup would be lower due to spatial variability of manure additions which cannot be accounted for in a 1-D model.

2.2.4 Soil

Input of plant litter expressed in terms of C of *v* that is transported to $\mathrm{C_d}$ ($\mathrm{C_0 = C_{labile}}$, $\mathrm{C_1 = C_{recalcitrant}}$) is expressed according to:

$$\left(\frac{\delta \mathrm{C}}{\delta t}\right)_{\mathrm{litter,d,v}} = \sum_{\mathrm{sl=0}}^{\mathrm{slMax}}\left(\mathrm{fr_{v,sl}}\cdot f_{\mathrm{d}}\cdot\rho \mathrm{Cr_v}\left(\frac{\delta \mathrm{Br_{sl}}}{\delta t}\right)_{\mathrm{turnover,v}}\right)+f_{\mathrm{d}}\cdot\rho\mathrm{Cs_v}\left(\frac{\delta \mathrm{Bs}}{\delta t}\right)_{\mathrm{turnover,v}}+\left(\frac{\delta \mathrm{C}}{\delta t}\right)_{\mathrm{harv\_litter,v}} \tag{18}$$

where $\mathrm{fr}_{v,\mathrm{sl}}$ is the fraction of root biomass of v in sl (derived from Eq. 12), f_d is the fraction of labile ($d = 0$) or recalcitrant ($d = 1$) constituents in turnover biomass, $\rho\mathrm{Cr}_\mathrm{v}$ and $\rho\mathrm{Cs}_\mathrm{v}$ are concentrations of C in root and shoot biomass ($\mathrm{g\,C\,g^{-1}}$ DW). Additions to the N pools are expressed similarly, where $\rho\mathrm{Nr}_\mathrm{v}$ (calculated dynamically) is applied instead of $\rho\mathrm{Cr}_\mathrm{v}$, $\rho\mathrm{Ns}_\mathrm{v}$ instead of $\rho\mathrm{Cs}_\mathrm{v}$, $\delta\mathrm{N}/\delta t$ instead of $\delta\mathrm{C}/\delta t$.

The OGM user can specify manure applications as inorganic N ($\mathrm{N_{inorg}}$ in $\mathrm{kg_N\,ha^{-1}}$), organic N ($\mathrm{N_{org}}$ in $\mathrm{kg_N\,ha^{-1}}$), and organic C ($\mathrm{C_{org}}$ in $\mathrm{kg_C\,ha^{-1}}$). Organic manure enters a C pool according to:

$$\left(\frac{\delta \mathrm{C}}{\delta t}\right)_{\mathrm{litter,d,sl=0}} = \mathrm{fm_d} \cdot \left(\frac{\delta \mathrm{C}}{\delta t}\right)_{\mathrm{manure}} \tag{19}$$

where $\mathrm{fm_d}$ is the fraction of a component ($d = 0, 1$ for labile and recalcitrant) in applied manure. Additions to $\mathrm{N_d}$ are calculated with a similar equation ($\mathrm{N_d}$ for $\mathrm{C_d}$). $\mathrm{N_{inorg}}$ is added to $\mathrm{Diss_{sl}}$ in the top layer ($\mathrm{sl} = 0$) of the soil:

$$\left(\frac{\delta \mathrm{N_{diss}}}{\delta t}\right)_{\mathrm{litter,sl=0}} = \left(\frac{\delta \mathrm{N}}{\delta t}\right)_{\mathrm{manure}} \tag{20}$$

Decomposition of C from a pool $\mathrm{C_d}$ is calculated according to:

$$\left(\frac{\delta \mathrm{C}}{\delta t}\right)_{\mathrm{dec,d,sl}} = K_\mathrm{d} \cdot \tau_\mathrm{sl} \cdot m_\mathrm{sl} \cdot \mathrm{C_{d,sl}} \tag{21}$$

where K_d is the potential decomposition rate of d, τ_sl and m_sl are temperature and moisture dependent decomposition rate reductions. Decomposition of $\mathrm{N_d}$ is calculated with a similar equation by replacing $\mathrm{N_d}$ for $\mathrm{C_d}$. Temperature-dependent rate reduction (τ_sl) is expressed as:

$$\tau_\mathrm{sl} = Q_{10}^{\left(\frac{T_\mathrm{sl} - T_\mathrm{OPT}}{10}\right)} \tag{22}$$

Where Q_{10} is the decomposition rate response to a 10 °C increase in temperature. T_OPT is the optimum decomposition temperature and T_sl is temperature of soil layer sl calculated in the temperature submodel (Fig. 1). The decomposition rate reduction factor associated with suboptimal soil moisture (m_{sl}) is expressed as:

$$m_{\mathrm{sl}} = \left(\frac{\theta_{\mathrm{sl}}}{\theta_{\mathrm{opt}}}\right)^{\lambda\mathrm{dec}} \tag{23}$$

where θ_{sl} and θ_{opt} are soil water content in soil layer sl, and the optimum soil water content for decomposition, respectively. λdec is a tuning parameter.

Leaching depends on the infiltration rate of moisture according to

$$\left(\frac{\delta \mathrm{N_{diss}}}{\delta t}\right)_{\mathrm{leaching,sl}} = f\cdot \mathrm{Fw_{sl}}\cdot \frac{\mathrm{N_{diss_{sl}}}}{h_{\mathrm{sl}}} \tag{24}$$

where $(\frac{\delta \mathrm{N_{diss}}}{\delta t})_{\mathrm{leaching,sl}}$ is $\mathrm{N_{diss}}$ that penetrates a deeper layer. $\mathrm{Fw_{sl}}$ is the rate of water infiltration in layer sl ($\mathrm{m\,s^{-1}}$), calculated in the water cycle module (Fig. 1), and f is a proportionality constant that expresses the fraction of N in $\mathrm{N_{diss_{,sl}}}$ that is mobile (i.e. nitrate/all species of dissolved N). Equation (24) quantifies leaching of N when sl = slMax. A constant fraction e of $\mathrm{N_{diss}}$ is lost as gaseous emission $(\frac{\delta \mathrm{N}}{\delta t})_{\mathrm{emission}}$.

$$\left(\frac{\delta \mathrm{N}}{\delta t}\right)_{\mathrm{emission,sl}} = e\cdot \mathrm{N_{diss_{sl}}} \tag{25}$$

Organic material slowly spreads due to bioturbation (i.e. mixing of material by soil animals). OGM assumes that the rate of transport of all litter types is equal, and decreases linearly with soil depth to 1 m:

$$\left(\frac{\delta \mathrm{C}}{\delta t}\right)_{\mathrm{pert,d,sl}} = c_{\mathrm{pert}}\cdot(1.0-\mathrm{depth_{sl}})\cdot \mathrm{C_{d,sl}} \tag{26}$$

where $\mathrm{C_d}$ expresses a C decomposition pool (labile or recalcitrant). Perturbation in the N pools ($\mathrm{N_d}$ for $d=\{0,1\}$) is described with a similar equation by replacing $\mathrm{C_d}$ by $\mathrm{N_d}$. $\mathrm{Depth_{sl}}$ is the distance from soil surface to the center of sl, and c_{pert} is the rate of perturbation at the surface.

2.3 Model application

2.3.1 Initialization

Soil initial conditions for the top 0–60 cm in INT and EXT were derived from site-specific measurements of soil properties. Measurements for the 4 soil parameters (bulk density, organic carbon fraction, C:N ratio and porosity) are available for the layers that represent soil depth 0–60 cm. These were used to initialize associated parameters in the model (i.e. the model was not set to equilibrium). An exponential fit was used to estimate soil properties in 60–100 cm depth from measurements in 0–60 cm depth. Uncertainty limits of vegetation and model parameters were derived from published values, and tuning parameters (notation $\lambda_{\text{specification}}$ in Sect. 2.2) were given uniform a-priori uncertainty ranges. Parameters such as altitude or heat properties of soil components remained fixed. We assumed that plant functional types (e.g. legumes and grasses) and site characteristics in INT and EXT were similar. Therefore, vegetation and model parameter values were equal.

2.3.2 Calibration

Uncertainty distributions were estimated for the different parameters that were previously described. In the context of this analysis, the use of a-priori knowledge was limited to estimates of minimum and maximum probable parameter values that are presented in literature. The model is applied repeatedly where parameter values are changed with each model call. Note that a model call in this context, consists of two simulations: INT and EXT. After each model call, the performance of the model was evaluated considering a suit of criteria for which information is available (e.g. soil moisture, root biomass, LAI, etc.). This performance was given a score, that is calculated as the sum of the coefficient of variation of RMSE ($\text{CV}_{\text{RMSE}} = \text{RMSE}/(x_{\max} - x_{\min})$ where $\text{RMSE} = \sqrt{}(\Sigma(y-x)^2/n)$, x = measured, y = modeled) over the criteria. The advantage of using CV_{RMSE} as a performance quantifier is that it is unit independent (allows a comparison of multiple criteria). When we present optimized model results, we were using parameter values that are associated with model calls that delivered the smallest value of ΣCV_{RMSE} in an extensive series (thousands) of model calls.

2.3.3 Evaluation

The model was evaluated using graphic comparisons of modeled and measured estimates. We further show normalized root mean square error (NRMSE) and coefficient of variation (R^2). NRMSE (=RMSE/$X_{average}$) to describe goodness-of-fit. NRMSE was used instead of CV_{RMSE}, because it is more commonly used in other literature, which allows a straightforward comparison with other models.

2.3.4 Climate and management scenarios

The climate change signal used to specify the scenarios was obtained from a simulation with the Climate High-Resolution Model (CHRM) (Vidale et al., 2003) completed in the framework of the PRUDENCE project (Christensen and Christensen, 2007). Corresponding changes in monthly precipitation amounts, average length of wet and dry spells, minimum and maximum temperature, temperature standard deviation and solar radiation nominally valid for the end of the 21st century already given in Lazzarotto et al. (2010) are reproduced here in Table 3 for the sake of clarity. Note that GSD was defined using only the changes in precipitation, amounts and average length of wet and dry spells from April to October.

Time series of synthetic daily weather data corresponding to the different scenarios, which were later adopted as an input to OGM, were developed using the LARSWG stochastic weather generator (Semenov, 2007). For our application, LARSWG was calibrated using 27 yr of high-quality daily weather observations spanning the period 1981–2007 from an operational weather station (Wynau, 7°47′ E, 47°15′ N, 422 m a.s.l.) close to our study site and provided by the Swiss Federal Office for Meteorology and Climatology (MeteoSwiss). For each of the three scenarios, the parameters defining the stochastic generation process were adjusted using the anomalies specified in Table 3 (for details see Semenov, 2007). These adjustments were assumed to be valid in 2100; linear interpolation in time was internally applied to infer a transient evolution of the monthly climate (Lazzarotto et al., 2010).

Ultimately, 110 yr of synthetic weather data were generated for each scenario. In addition, a 110-yr time series was also generated without modification of the calibration parameters. This simulation provides data statistically consistent with the current climate and was used in the so-called EQUIL runs (Table 4). We further used changes in the precipitation regime during April to October (Growing Season Drought, GSD) or changes in precipitation, temperature and solar radiation (A2-370), both with atmospheric CO_2 concentration fixed at 370 ppm, or changes in climate and CO_2 concentratiqons increasing to 860 ppm by 2100 (A2-860) according to predictions of atmospheric CO_2 by the Bern-CC model for the A2 emission pathway (see Appendix I in IPCC, 2000).

Management events were forecast for each year in the period 2010–2100, by randomly picking a year between 2001 and 2010, and assuming that the recorded harvest/manuring events in this year are repeated in the forecast year. Combining two management scenarios (INT/EXT) and four scenarios for climatic change (EQUIL/GSD/A2-370/A2-860), delivered 8 model runs (Table 4). Linear Regression lines were fit to the last decade of soil C to determine sequestration, where soil C at 1 January 2001 and its fitted value in 2101 were used as indicators.

3 Results

3.1 Model evaluation and performance (2002–2010)

Coefficients of determination (R^2) of soil temperature ranged from 0.97 to 0.99. Normalized root mean squared error (NRMSE) ranged from 0.05 to 0.07 °C (Table 5). Coefficients of determination (R^2) of soil moisture ranged from 0.77 at 5 cm depth to 0.89

at 10 cm depth (Table 5; Fig. 2). NRMSE indicated a similar goodness of fit across different soil depths, with the best fit at 30 cm depth (NRMSE = 0.11 %), and the least fit at 50 cm depth (NRMSE = 41 %). Dry periods in the summers were usually well captured by the model. We did find however, that the level of moisture extraction tended to be slightly underestimated in top soil, while overestimated in deeper soil (compare 5 and 10 cm soil depth with 30 and 50 cm soil depth in Fig. 2).

Legumes contributed ∼22 % to LAI in EXT (average for 100 yr), typically fluctuating between ∼5 % and ∼35 % (Fig. 3). With time, legumes died out in INT, in agreement with the situation in the field where clover had to be re-sown in 2006. The first harvest in each year was commonly underestimated and subsequent cuts were slightly overestimated due to an effect of growth stage (vegetative growth vs. reproductive growth) that is not implemented in the model. Additionally, the use of a constant harvest efficiency caused inadequate prediction of the extraction with individual cuts (for a review of harvest efficiency, see Ammann et al., 2007). The introduction of seasonal variability in growth rates and harvest efficiency could improve model predictions here, even though such inclusion would involve estimation of several additional model parameters.

Modeled root biomass approximated measured amounts in 2004 (Fig. 3; Table 5). Although not directly verified, there are indications that seasonal dynamics were plausible. For instance, Garcia-Pausas et al. (2011) measured maximum seasonal fluctuations in grass root biomass of approximately 30 % in a Pyrenees mountain grassland (compare with Fig. 3).

Aboveground litter production was 527–585 g DW m^{-2} yr^{-1} (EXT-INT), which was high compared to data from Hitz et al. (2001) who found values of 80–400 g C m^{-2} yr^{-1} in grasslands that produce 100 to 300 g DW m^{-2} with individual harvests. Note that aboveground litter here, does not include harvest remnants. Belowground litter production was 758–809 g DW m^{-2} yr^{-1} (EXT-INT).

Turnover time of grass roots was 1.4 yr, whereas Van der Krift and Berendse (2002) estimated root turnover times for some typical grass species (*Lolium perenne, Arrhenatherum elatius, Molinia caerulea, Nardus stricta*) in the range from 0.8 to 1.11 yr.

Longer turnover times (3.3–11.5 yr) were found in sub-alpine and alpine grasslands by Hitz et al. (2001).

3.1.1 Distribution of roots and soil C (2001–2006)

Root biomass in 2004 was slightly underestimated in EXT (modeled: 0.47 kg DW m^{-2}; measured 0.49 kg DW m^{-2}) and in INT (modeled: 0.52 kg DW m^{-2}; measured 0.58 kg DW m^{-2}). It was particularly underestimation in the topsoil (0–5 cm, modeled: 5.9 $mg_{DW}\,g_{soil}^{-1}$; measured 7.1 ± 5.2 $mg_{DW}\,g_{soil}^{-1}$), whereas root biomass density in EXT in the topsoil (0–5 cm) was slightly overestimated (modeled: 5.3 $mg_{DW}\,g_{soil}^{-1}$; measured 4.0 ± 3.3 $mg_{DW}\,g_{soil}^{-1}$). Note, however, that measurement errors in root biomass typically exceed lack-of-fit of the model.

Soil organic Carbon (0–45 cm) in 2006 was slightly underestimated in INT (modeled: 14.7 kg m^{-2}); measured: 14.8 ± 1.4 kg m^{-2}), and overestimated in EXT (modeled: 15.3 kg m^{-2}; measured 14.3 kg m^{-2}).

Modeled carbon concentration in INT had increased from 3.14 to 5.85 % (EXT) and from 3.10 to 4.04 % (INT) in the upper 5 cm, from 3.15 to 3.28 % (EXT) and from 3.05 to 3.16 (INT) between 5–10 cm depth. Small decreases were modeled in deeper layers (upto 0.14 %) in both INT and EXT, modeled losses were maximum in both sites at 10–20 cm depth. The distribution of C across depth was well captured by the model (R^2 = 0.99, RMSE = 0.13–0.21 INT/EXT). Concentrations of C increase in the top 10 cm of soil, but decreased below 10 cm during 10 yr of simulation.

3.1.2 Carbon balance (2001–2010)

The model was accurate for cumulative and inter-seasonal NEE in INT (Table 5), which indicated that the magnitude of NPP, respiration and cumulative NPP + respiration over time were simulated accurately. Cumulative CO_2 fluxes were overestimated by 25 % in EXT. Harvests were slightly underestimated in EXT but overestimated in INT. Soil in EXT started to lose C approximately 3 yr after establishment. These losses had not stabilized in 10 yr. Biomass reached a long-term average of 714 g DW m^{-2} in EXT (belowground biomass: 620 g DW m^{-2}; aboveground biomass: 94 g DW m^{-2}) and 751 g DW m^{-2} in INT (belowground biomass: 664 g DW m^{-2}; aboveground biomass: 87 g m^{-2}) after approximately 4 to 5 yr (EXT and INT). Yet, stabilization of soil C was not completed until several decades in both INT and EXT (see Sect. 3.2.).

3.2 Carbon sinks in 2001–2100

Differences in soil C between climate scenarios became evident approximately 20 yr after establishment (Fig. 5). Scenarios that involved increasing concentrations of atmospheric CO_2, in particular A2-860, led to higher soil C than the stable climate scenario (EQUIL). Differences between GSD/A2-370 scenarios and EQUIL occurred later. In INT, soil C accumulated until approximately 45 yr after establishment. In EXT, losses of C were predicted to continue throughout the century and for all climate scenarios, except A2-860 for which soil C loss stopped after 50 yr and increased until the end of simulation. INT accumulated C during the first 45 yr after establishment, and soil C remained nearly constant with all scenarios except with INT/A2-860 where C accumulated throughout the century. With the EQUIL scenario, soil C in EXT continued declining after 45 yr, but the loss slowed down after 2045.

This period of stabilization was independent of climate scenario (Fig. 5). As biomass stabilized, changes in soil C were increasingly dominated by climatic effects. Towards the end of the simulation, C dynamics were effectively dominated by vegetation responding to different climatic drivers.

Compared to EQUIL, NPP was lower in precipitation scenarios (INT/GSD: −3.4 %, EXT/GSD: −4.4 %). NPP increased in precipitation, temperature and radiation scenarios (INT/A2-370: 3.1 %, EXT/A2-370: 3.4 %) and increased in climate + atmospheric CO_2 scenarios as well (INT/A2-860: 19.2 %, EXT/A2-860: 25.2 %). Harvested biomass was lower by a similar fraction in either management system in a precipitation scenario (INT/GSD: −5.4 %, EXT/GSD: −5.2 %). Slightly higher harvests were predicted for scenarios that involved warming, higher radiation and lower precipitation (INT/A2-370: 3.1 %, EXT/A2-370: 3.5 %). Considerable increases were found for scenarios that involved higher atmospheric CO_2 together with changed climatic conditions (INT/A2-860: 7.5 %, EXT/A2-860: 14.2 %).

Respiration decreased in precipitation scenarios (INT/GSD: −2.4 %, EXT/GSD: −3.4 %), but was higher in the other scenarios (INT/A2-370: 4.1 %, EXT/A2-370: 5.1 %, INT/A2-860: 7.5 %, EXT/A2-860: 14 %).

Net C sequestration was predicted for all of the INT scenarios (INT/EQUIL: 1.3 g C m^{-2}, INT/GSD: $1.2 \pm 0.1\ \text{g C m}^{-2}$, INT/A2-370: $1.8 \pm 0.2\ \text{g C m}^{-2}$, INT/A2-860: $5.3 \pm 0.3\ \text{g C m}^{-2}$). Losses of soil C resulted for all EXT scenarios except EXT/A2-860 (EXT/EQUIL: $-3.1\ \text{g C m}^{-2}$; EXT/GSD: $-3.9 \pm 1.1\ \text{g C m}^{-2}$; EXT/A2-370: $-2.1 \pm 0.3\ \text{g C m}^{-2}$, EXT/A2-860: $1.6 \pm 0.3\ \text{g C m}^{-2}$). Across all climate scenarios, there was a consistent and considerable difference between soil C sequestration in EXT and INT. Harvest and Respiration were tightly coupled to NPP in all the climate scenarios, the ratio of harvest/NPP (in kgC kgC^{-1}) over the total simulation period ranged from 27–30 % in EXT and 29–32 % in INT (Fig. 5). Similarly, respiration/NPP ranged from 71–75 % in EXT and from 71–74 % in INT. Low respiration/NPP and harvest/NPP ratios were typically found for A2-860 in both INT and EXT. Highs were not so consistent, with maxima for both harvest and precipitation in an A2-GSD scenario (INT), but in EQUIL for harvest and A2-370 for respiration (EXT).

Distribution of roots and soil C in 2001–2100

Soil C increased mainly in the top 15 cm of the soil, whereas small losses occurred from 15 to 85 cm. Losses of C in EXT/EQUIL stabilized after approximately 50 yr. Until then, the model simulated C losses to occur particularly between 15 and 80 cm depth (Fig. 4), summing up to ∼1.5 kg C m^{-2} over the entire 100-yr simulation period. Hence, with time the range of depth where soil C loss occurred shifted slightly downward (compare Fig. 4 with Fig. 6).

4 Discussion

4.1 Long-term SOC

Our simulation results indicate that SOC stabilizes in EQUIL and GSD for INT, even though C loss in EXT had not come to a halt in 2100. ΔSOC after land use conversion, depends particularly on the balance of litter production, manure, and decomposition rates. Litter production depends on moisture and temperature, but also on seasonal aspects such as foliage cover, root density, growth and harvest efficiency. After a land use change, we can expect that litter production changes with growth rate. Decomposition of SOC depends foremost on a-biotic conditions, quality and quantity of litter. SOC will therefore tend to increase or decrease depending on the new balance between littering and decomposition, until it stabilizes when the level of SOC has changed to such extend that littering and manure input equals decomposition.

The level of SOC at which saturation occurs is of importance to explain our simulation results. We found $\Delta\text{SOC} = 7.0\,\%$(INT) and $-14.7\,\%$(EXT), values that are lower than those given either by Poeplau et al. (2011) or IPCC (2000, Table 1). While Poeplau et al. (2011) and IPCC (2000) review studies of lands that are exclusively managed in arable rotations, Oensingen had been under ley-arable management. Leifeld et al. (2005) found substantially higher SOC in ley-arable managed soil. The Oensingen sites contained 18–20 kg C m^{-2} prior to conversion while IPCC (2000) assumes $\text{SOC} = 8\,\text{kg C m}^{-2}$ for croplands and arable soils that were considered by Poeplau et al. (2011) contained merely $4.6 \pm 2.1\,\text{kg C m}^{-2}$. High SOC in ley-arable managed soil may be due particularly to high litter input in rotations of grassland and seasons in which the field remained unused. Because litter input may have been of similar quantity prior to land use change, sequestration potentials with conversion to permanent grassland, may have depended strongly on manure-C input (see also Sect. 4.2).

We can also compare our results with those found by Riedo et al. (2000), who modeled 3 sites with typical characteristics: Bern (high productivity), Sion (dry), and Davos (high altitude). The PaSim model was used to estimate sequestration potentials under different management options (cutting or grazing) and climates. Assuming a scenario comparable with our A2-860 scenario (lower precipitation, higher temperatures, radiation intensity and concentrations of atmospheric CO_2; T2pm) Riedo et al. (2000) found that soil C decreased by ∼5 % for Bern and ∼10 % for Sion, but increased ∼13 % for Davos, relative to a reference simulation (T0P0) that involved higher atmospheric CO_2 alone.

Our reference climate scenario (EQUIL) assumes that atmospheric CO_2 concentrations remain constant, so we ran an additional simulation using a climate scenario in which only atmospheric CO_2 increases, but temperature, precipitation and radiation remain constant. We found 4.4 % in INT (0.8 kg C m^{-2}) and 4.8 % in EXT (1.0 kg C m^{-2}) lower C contents compared to the reference scenario, which is very similar to results Riedo et al. (2000) found for Bern.

Our estimate indicates a sink of 0.06 kg C m^{-2} in INT based on the difference between INT and EXT after 100 yr. In comparison, Lal (2007) estimated that introducing fertilization creates a sink for C of only 0.01–0.02 kg C m^{-2} yr^{-1} on average, or conversion of arable land to pasture, a sink of 0.04–0.06 kg C m^{-2} yr^{-1}. While our findings in INT are very comparable with studies reviewed in Lal (2007), we found substantially lower sequestration potentials in EXT.

If we use linear extrapolation to estimate ΔSOC in 2100, we find a loss of ∼3 kg C m^{-2} by 2100 in INT and a similar accumulation in EXT. Hence while ΔSOC is near to constant in EXT/EQUIL during 2001–2100, it decreases in INT. Therefore, our long-term simulations indicate that the tendency observed during the first 10 yr cannot generally be extrapolated beyond approximately 20 yr. This has implications for the interpretation of field experiments that attempt to quantify possible long-term changes in SOC stock by sampling soil profiles over shorter time intervals.

We found that C accumulation initially occurs mainly in the top 10 cm of the soil, but increases to ∼15 cm in the course of 100 yr simulation. In agreement, Conant et al. (2001) found that SOC increments were observed particularly in the top 10 cm soil. It is very common that SOC is not measured beyond 30 cm. In fact, the average soil depth in studies reviewed by Conant et al. (2001) was only 32.2 cm. However, we investigated how ΔSOC changes with soil depth (Fig. 6), and we found indications that C sequestration potentials need to consider deeper layers, as root littering increases with root depth and the density of root biomass in greater depth. The change in SOC with depth is considerable in the top 50 cm of the soil at least, and the simulations suggest C loss to occur below 40 cm depth in the EXT/EQUIL scenario, and C gains above. Hence considerable changes in C sequestration potentials can occur at levels deeper than are commonly measured, although depending on site management and history, the potentials for C accumulation at >30 cm soil depth may be small.

4.2 The importance of biomass turnover and manure type

We found that C sequestration potentials differ considerably according to management intensity. In more detail, two processes are particularly important: biomass turnover and manure application.

The assumption that vegetation characteristics for a cohort (grass or clover) are the same regardless of management was inevitable because vegetation developments in INT and EXT would be equally well explained by plant characteristics (e.g. water use efficiency, biomass growth response to soil N) as by abiotic conditions (soil water content, dissolved N in the soil) if vegetation parameters had been allowed to vary freely. However inevitable, this assumption introduces some uncertainties. The seed mixture that was used in EXT for example, contained different and more species of grasses than the mixture that was used in INT, and also contained herbs.

The use of equal biomass turnover rates in INT and EXT in particular, may lead to an overestimation of biomass senescence, and SOC, in EXT for which measured cumulative NEE was ~25 % higher than modeled NEE (Table 5: compare overestimation in EXT: NEE with underestimation in EXT: harvest). This overestimation is related to a considerable difference in "Sequestration efficiency" ($S_e = 1.0 - \text{harvest/NEE}$). between INT and EXT. Measurements indicate that S_e is considerably lower in EXT (0.15) than in INT (0.44), whereas this ratio is near to constant in the simulations (EXT: 0.37, INT:

Title Page
Abstract Introduction
Conclusions References
Tables Figures
◀| |▶
◀ ▶
Back Close
Full Screen / Esc
Printer-friendly Version
Interactive Discussion

0.40). This difference is consistent with a slight underestimation (0.1 kg C m^{-2}) of soil C in 2006 in INT, and a considerable overestimation (1.0 kg C m^{-2}) of modeled SOC in 2006 in EXT. Hence it is unlikely that this lack of fit is related to measurement uncertainty.

This finding is unexpected because litter in unfertilized (nitrogen poor) grassland is generally thought to decompose slower (Aerts et al., 2003). Instead a converse effect seems to dominate in EXT. For example, higher aboveground allocation could be sustained due to lower (belowground) senescence. There are two known plant adaptations to nutrient poor conditions that lead to reduced senescence in nutrient poor conditions (Chapin, 1980; Loualt et al, 2005). One response is instantaneous: senescence of both root and shoot increases with protein concentration in the plant tissues. Moreover, root longevity may be extended due to mycorrhizal symbiosis that is stronger in nutrient poor conditions. A second response is genetic: slow-growing species are better capable to compete in nutrient poor conditions by increased longevity of biomass (Chapin, 1980).

Manure application increases soil C indirectly, via higher plant assimilation and litter production, as well as directly through manure-C amendment (Leifeld and Fuhrer, 2010; Jones et al., 2006). We tested how these two mechanisms contribute to the difference that we found with four slightly different model applications. Excluding manure-derived C from our INT/EQUIL simulation (Table 4; i.e. manure-N is spread among soil deposition pools according to Eq. 18) would lead to a 1.0 kg C m^{-2} lower soil C after 100 yr (i.e. it reduces C increment from 1.1 to 0.1 kg C m^{-2}). A similar difference is found when all manure-bound N is applied with inorganic fertilizer (ΔSOC = ~0.0). The results indicate that ~60 % of the manure effect on soil C over a 100-yr simulation can be attributed to import of C.

5 Conclusions

We have analyzed how management and global warming interact in two grassland systems established on former cropland in Central Switzerland. The aim was to investigate the long-term relationship between climate, soil C storage and management during a 100-yr simulation period following establishment in 2002. The simulation results lead to the following conclusions:

1. Intensive management (i.e. fertilization) dominates the SOC stock until ∼45 yr after sowing, while climate change dominates soil C in the longer term.
2. Previous arable land use has to be specified exactly to estimate potential sequestration of C is low. Prior to conversion, Oensingen grasslandse had high SOC due to the use of ley-arable rotations as compared to an exclusively arable cropping system.
3. A larger fraction of the increase in soil organic C in fertilized plots originates from applied manure, compared to the input from increased amounts of plant litter.
4. After establishment, soil C increases mainly in the top 10 cm of soil, but in the course of 100 yr, soil C increments are observed down to 15 cm.
5. Comparing the Oensingen site with conditions that are dominant in Switzerland, C sequestration potentials may be lower at warm, low precipitation sites, but higher at cooler and wet high-altitude sites.

Acknowledgements. This work was funded by the Swiss national Science Foundation in the framework of the NCCR Climate project AGRISK. We further thank Mikhail Semenov for the use of his LARS Weather Generator, as well as MeteoSwiss for making climate records publically available.

References

Aerts, R., De Caluwe, H., and Beltman, B.: Plant community mediated vs. nutritional controls on litter decomposition rates in grasslands, Ecology, 84, 1398–3208, 2003.

Aeschlimann, U., Nösberger, J., Edwards, T. J., Schneider, M. K., Richer, M., and Blum, H.: Responses of net ecosystem CO_2 exchange in managed grassland to long-term CO_2 enrichment, N fertilization and plant species, Plant Cell Environ., 28, 823–833, 2005.

Ainsworth, E. A., Davey, P. A., Hymus, G. J., Osborne, C. E., Rogers, A., Blum, H., Nosberger, J., and Long, S. E.: Is stimulation of leaf photosynthesis by elevated carbon dioxide concentration maintained in the long term? A test with Lolium perenne grown for 10 years at two nitrogen fertilization levels under Free Air CO_2 Enrichment (FACE), Plant Cell Environ., 26, 705–714, 2003.

Ammann, C., Flechard, C. R., Leifeld, J., Neftel, A., and Fuhrer, J.: The carbon budget of newly established grassland depends on management intensity, Agr. Ecosyst. Environ. 121, 5–20, 2007.

Ammann, C., Spirig, C., Leifeld, J., and Neftel, A.: Assessment of the nitrogen and carbon budget of two managed temperate grassland fields, Agr. Ecosyst. Environ., 133, 150–162, 2009.

Casella, E. and Soussana, J.-F.: Long-term effects of CO_2 enrichment and temperature increase on the carbon balance of a temperate grass sward, J. Exp. Bot., 48, 1309–1321, 1997.

Chapin, F. S.: The mineral nutrition of wild plants, Annu. Rev. Ecol. Syst., 11, 233–260, 1980.

Christensen, J. H. and Christensen, O. B.: A summary of the PRUDENCE model projections of changes in European climate by the end of this century, Climatic Change, 81, 7–30, 2007.

Conant, R. T., Paustian, K., and Elliot, E. T.: Grassland management and conversion into grassland: effects on soil Carbon, Ecol. Appl., 11, 343–355, 2001.

Conant, R. T., Ogle, S. M., Paul, E. A., and Paustian, K.: Measuring and monitoring soil organic carbon stocks in agricultural lands for climate mitigation, Front Ecol. Environ., 9, 169–173, 2011.

De Bruijn, A. M. G. and Butterbach-Bahl, K.: Linking carbon and nitrogen mineralization with microbial responses to substrate availability – the DECONIT model, Plant Soil, 328, 271–290, 2010.

De Bruijn, A. M. G., Butterbach-Bahl, K., and Grote, R.: Model evaluation of different mechanisms driving freeze-thaw N_2O emissions, Agr. Ecosyst. Environ., 3–4, 196–207, 2009.

FAO, ISRIC and ISSS: World Reference Base for Soil Resources, Food and Agriculture Organization of the United Nations, Rome, 1998.

Garcia-Pausas, J., Casals, P., Romanyà, J., Vallecillo, S., Sebastià, M.-T.: Seasonal patterns of belowground biomass and productivity in mountain grasslands in the Pyrenees, Plant Soil, 340, 315–326, 2011.

Gerwitz, A. and Page, E. R.: An empirical mathematical model to describe plant root systems, J. Appl. Ecol., 11, 773–782, 1974.

Hitz, C., Egli, M., and Fitze, P.: Below-ground and above-ground production of vegetational organic matter along a climosequence in alpine grasslands, J. Plant Nutr. Soil Sci., 164, 389–397, 2001.

IPCC: Climate Change 2007: The Physical Science Basis. Contribution of Working Group I to the Fourth Assessment Report of the Intergovernmental Panel on Climate Change, edited by: Solomon, S., Qin, D., Manning, M., Chen, Z., Marquis, M., Averyt, K. B., Tignor, M., and Miller, H. L., Cambridge University Press, Cambridge, United Kingdom and New York, NY, USA, 996 pp., 2007.

IPCC: Land use, land use change, and forestry. Intergovernmental Panel on Climate Change: a special report of the IPCC, Cambridge University Press, Cambrindge, 2000.

Jones, S. K., Rees, R. M., Kosmas, D., Ball, B. C., and Skiba, U. M.: Carbon sequestration in a temperate grassland: management and climatic controls, Soil Use Manage., 22, 132–142, 2006.

Jenkinson, D. S., Adams, D. E., and Wild, A.: Model estimates of CO_2 emissions from soil in response to global warming, Nature, 351, 304–306, 1991.

Jentsch, A., Kreyling, J., Elmer, M., Gellesch, E., Glaser, B., Grant, K., Hein, R., Lara, M., Mirzae, H., Nadler, S. E., Nagy, L., Otieno, D., Pritsch, K., Rascher, U., Schädler, M., Schloter, M., Singh, B. K., Stadler, J., Walter, J., Wellstein, C., Wöllecke, J., and Beierkuhnlein, C.: Climate extremes initiate ecosystem-regulating functions while maintaining productivity, J. Ecol., 99, 689–702, 2011.

Kätterer, T., Reichstein, M., Andrén, O., Lomander, A., and Andrén, O.: Temperature dependence of organic matter decomposition: a critical review using literature data analyzed with different models, Biol. Fertil. Soils, 27, 258–262, 1998.

Kesik, M., Ambus, P., Baritz, R., Brüggemann, N., Butterbach-Bahl, K., Damm, M., Duyzer, J., Horváth, L., Kiese, R., Kitzler, B., Leip, A., Li, C., Pihlatie, M., Pilegaard, K., Seufert, S., Simpson, D., Skiba, U., Smiatek, G., Vesala, T., and Zechmeister-Boltenstern, S.: Inventories of N_2O and NO emissions from European forest soils, Biogeosciences, 2, 353–375, doi:10.5194/bg-2-353-2005, 2005.

Kulshreshtha, S. and Sobool, D.: Comparative Greenhouse Gas Emission Intensities from Irrigated and Dryland Agricultural Activities in Canada, Canadian Water Res. J., 31, 157–172, 2006.

Lal, R.: Carbon management in agricultural soils, Mitig. Adapt. Strat. Global Change, 12, 303–322, 2007.

Lazzarotto, P., Calanca, P., Semenov, M., and Fuhrer, J.: Transient responses to increasing CO_2 and climate change in an unfertilized grass-clover sward, Clim. Res., 41, 221–232, 2010.

Lee, M., Manning, P., Rist, J., Power, S. A., and Marsh, C.: A global comparison of grassland biomass responses to CO_2 and Nitrogen enrichment, Phil. Trans. R. Soc. B, 365, 2047–2056, 2010.

Leifeld, J. and Fuhrer, J.: Organic farming and soil carbon sequestration: What do we really know about the benefits?, AMBIO, 39, 585–599, 2010.

Leifeld, J., Bassin, S., and Fuhrer, J.: Carbon stocks in Swiss agricultural soils predicted by land-use, soil characteristics, and altitude, Agr. Ecosyst. Environ., 105, 255–266, 2005.

Li, C., Frolking, S., and Frolking, T. A.: A model of nitrous oxide evolution from soil driven by rainfall events: 1. Model structure and sensitivity, J. Geophys. Res., 97, 9759–9776, 1992.

Louault, F., Pillar, V. D., Aufrère, J., Garnier, E., and Soussana, J.: Plant traits and functional types in response to reduced disturbance in a semi-natural grassland, J. Veg. Sci., 16, 151–160, 2005

Morecroft, M. D., Masters, G. J., Brown, V. K., Clarke, I. P., Taylor, M. E., and Whitehouse, A. T.: Changing precipitation patterns alter plant community dynamics and succession in an ex-arable grassland, Funct. Ecol., 18, 648–655, 2004.

Müller, C.: Modelling Soil-Biosphere Interactions, CAB International, New York, 2000.

Nijs, I., Impens, I., and Behaeghe, T.: Leaf and canopy responses of Lolium perenne to long-term elevated atmospheric carbon-dioxide concentration, Planta, 177, 312–320, 1989.

Parton, W. J., Schimel, D. S., Cole, C. V., and Ojima, D. S.: Analysis of factors controlling soil organic matter levels in Great Plains grasslands, Soil Sci. Soc. Am. J., 51, 1173–1179, 1987.

Poeplau, C., Don, A., Vesterdal, L., Leifeld, J., van Wesemael, B., Schumacher, J., and Gensior, A.: Temporal dynamics of soil organic carbon after land-use change in the temperate zone – carbon response functions as a model approach, Glob. Change Biol., 17, 2415–2427, 2011.

Priestley, C. H. B. and Taylor, R. J.: On the assessment of surface heat flux and evaporation using large-scale parameters, Mon. Weather Rev., 100, 81–82, 1972.

Riedo, M., Grub, A., Rosset, M., and Fuhrer, J.: A pasture simulation model for dry matter production, and fluxes of carbon, nitrogen, water and energy, Ecol. Model., 105, 141–183, 1998.

Riedo, M., Gyalistras, D., and Fuhrer, J.: Net primary production and carbon stocks in differently managed grasslands: simulation of site-specific sensitivity to an increase in atmospheric CO_2 and to climate change, Ecol. Model., 134, 207–227, 2000.

Ryle, G. J. A., Weledge, J., Tewson, V., and Powell, C. E.: Influence of Elevated CO_2 and Temperature on the Photosynthesis and Respiration of White Clover Dependent on N_2 Fixation, Ann. Bot., 70, 213–220, 1992.

Schapendonk, A. H. C. M., Dijkstra, P., Groenwold, J., Pot, C. S., and van de Gijn, S. C.: Carbon balance and water use efficiency of frequently cut Lolium perenne swards at elevated carbon dioxide, Glob. Change Biol., 3, 207–216, 1997.

Schimel, D. S.: Terrestrial ecosystems and the carbon cycle, Glob. Change Biol., 1, 77–91, 1995.

Semenov, M. A.: Development of high resolution UKCIP02-based climate change scenarios in the UK, Agr. Forest Meteorol., 144, 127–138, 2007.

Steduto, P., Hsiao, T. C., Raes, D., and Fereres, E.: AquaCrop – The FAO crop model to simulate yield response to water: I Concepts and underlying principles, Agron. J., 101, 426–437, 2009.

Thornley, J. H. M. and Johnson, I. R.: Plant and Crop Modeling, Clarendon Press, Oxford, 1990.

Van der Krift, T. A. J. and Berendse, F.: Root life spans of four grass species from habitats differing in nutrient availability, Funct. Ecol., 16, 198–203, 2002.

Van Wesemael, B., Paustian, K., Meersmans, J., Goidts, E., and Barancikove, G.: Agricultural management explains historic changes in regional soil carbon stocks, P. Natl. Acad. Sci. USA, 107, 14926–14930, 2010.

Vidale, P. L., Lüthi, D., Frei, C., Seneviratne, S., and Schär, C.: Predictability and uncertainty in a regional climate model, J. Geophys. Res., 108, 4586, doi:10.1029/2002JD002810, 2003.

Wand, S. J. E., Midgley, G. F., Jones, M. H., and Curtis, P. S.: Responses of wild C4 and C3 grass (Poaceae) species to elevated atmospheric CO_2 concentration: a meta-analytic test of current theories and perceptions, Glob. Change Biol., 5, 723–741, 1999.

Xu, X., Liu, W., and Kiely, G.: Modeling the change in soil organic carbon (SOC) of grassland in response to climate change: effects of measured versus modeled carbon pools for initializing RothC model, Agr. Ecosyst. Environ., 140, 372–381, 2011.

Zeeman, J. M.: Environmental processes affecting the carbon dioxide budget of grasslands along an elevational gradient in Switzerland, Doctoral Thesis, ETH Zurich, http://e-collection.ethbib.ethz.ch/view/eth:41494, 2008.

Table 1. Literature estimates of ΔSOC with land use conversions from arable to pasture or management intensivation in terms of manure applications and ploughing frequency.

	Author	ΔSOC	Period	Remark
Arable soil to pasture	IPCC, 2000	+100 %	long term	Static estimates of stable C in different land use types: 8 kg C m^{-2} in arable soil, 23 kg C m^{-2} in grassland
	Poeplau et al. (2011)	+39.8 ± 11 %	20 yr	Based on 24 studies/89 datapoints
		+128 ± 23 %	100 yr	Based on 24 studies/89 datapoints
	Lal (2007)	+400–600 kg ha^{-1}	1 yr	
	Conant et al. (2001)	1010 kg ha^{-1}	1 yr	Conversion: cultivation to pasture (23 datapoints)
	Ammann et al. (2007)	1470 ± 1300 kg ha^{-1}	1 yr	Intensive management (INT) as in this manuscript
		−570 (+1300/−1100) kg ha^{-1}	1 yr	Extensive management (EXT) as in this manuscript
Intensification	Lal (2007)	100–200 kg ha^{-1}	1 yr	West and Post (2002) in Lal (2007)
	Conant et al. (2001)	300 kg ha^{-1}	1 yr	Fertilization (42 datapoints)

Table 2. Measurements taken in the context of the Oensingen experiments, used in this study (Ammann et al., 2007, 2009).

Measurement	Time span	Management
Air temperature	1981–2010	INT+EXT
Precipitation	1981–2010	INT+EXT
Soil temperature	2002–2010	INT
Soil moisture	2002–2010	INT
Root biomass	2004	INT+EXT
Leaf area index (LAI)	2003–2010	INT+EXT
Soil C/N ratio, bulk density, porosity, organic C	2002	INT+EXT
Soil-atmosphere CO_2 exchange	2002–2010	INT+EXT
Manure application	2002–2010	INT
Cut biomass	2002–2009	INT+EXT
Harvested biomass	2002–2009	INT+EXT

Table 3. Changes (Δ) in monthly climate statistics between 2071–2100 and 1961–1990 simulated by the Climate High Resolution Model for the Swiss Plateau under the assumption of an A2 emissions scenario. Changes in mean precipitation rate (P), duration of wet (τ_{wet}) and dry (τ_{dry}) spells, global radiation (GR) and interannual standard deviation of air temperature (σT) are relative; changes in daily maximum (T_{max}) and minimum (T_{min}) air temperature are absolute.

Month	ΔP	$\Delta\tau_{wet}$	$\Delta\tau_{dry}$	ΔT_{max} (C)	ΔT_{min} (C)	$\Delta\sigma T$	ΔGR
Jan	1.1	0.91	0.65	3.51	3.07	0.8	1.07
Feb	1.44	1.19	0.73	2.57	2.11	0.79	0.98
Mar	1.26	1.01	0.7	1.93	1.38	0.96	1
Apr	0.99	0.86	1.11	2.99	2.15	1.18	1.14
May	0.77	0.53	1.23	3.58	2.49	1.11	1.16
Jun	0.72	0.72	1.75	4.07	2.89	1.33	1.13
Jul	0.53	0.77	2.21	5.64	3.49	1.23	1.14
Aug	0.69	0.75	1.79	7.05	4.28	1.13	1.17
Sep	0.72	0.86	1.34	5.95	4	1	1.12
Oct	0.98	0.81	1.08	4.4	3	1.11	1.16
Nov	0.66	0.82	1.34	3.39	1.64	0.96	1.32
Dec	1.06	1.15	0.92	3.37	2.58	0.79	1.23

Table 4. Climate scenarios (reps. for randomized realizations of a climate scenario).

#	Scenario	Climate scenario	Period	Reps
1	EQUIL	Climate equilibrium	2010–2100	1
2	GSD	Growing season drought	2010–2100	5
3	A2-370	Full A2 climate scenario, but with CO_2 concentration kept constant at 370 ppm	2010–2100	5
4	A2-860	Full A2 climate scenario, with CO_2 concentration reaching 860 ppm by the end of the century	2010–2100	5

Table 5. Model performance on soil temperature, soil moisture, biomass and ΔSOC. Note that only pairs of modeled and measured values are included in cumulative and average values to facilitate comparisons. Sums of measured NEE, gap-filled with annual averages are shown in brackets. Criteria for goodness of fit are given when $n > 1$.

Variable		Average		Cumulative		Goodness of fit	
		measured	modeled	measured	modeled	R^2	NRMSE
Temperature 2 cm (°C)	INT	10.6	10.6	–	–	0.97	0.06
Temperature 5 cm (°C)	INT	10.6	10.6	–	–	0.98	0.05
Temperature 10 cm (°C)	INT	10.6	10.6	–	–	0.98	0.05
Temperature 30 cm (°C)	INT	10.7	10.7	–	–	0.98	0.05
Temperature 50 cm (°C)	INT	10.6	10.7	–	–	0.97	0.07
Moisture 5 cm (%VOL)	INT	38.6	42.4	–	–	0.77	0.16
Moisture 10 cm (%VOL)	INT	40.9	42.1	–	–	0.89	0.12
Moisture 30 cm (%VOL)	INT	43	42.7	–	–	0.87	0.11
Moisture 50 cm (%VOL)	INT	44.1	41.9	–	–	0.82	0.41
LAI ($m^2\ m^{-2}$)	INT	2.06 ± 0.45	2.15	–	–	0.35	0.26
	EXT	2.03 ± 0.61	1.98	–	–	0.61	0.19
Abg biom at harvest g DW m^{-2}	INT						
	EXT	253.9 ± 166.7	243.8 ± 91.6				
Long-term clover dominance	INT	–	0 %	–	–	–	–
	EXT	–	22 %	–	–	–	–
Root mass profile 2004 (mg g^{-1} DW)	INT	1.55 ± 1.01	1.28	–	–	0.99	0.57
	EXT	1.01 ± 0.76	1.14	–	–	0.99	0.54
Root biomass 2004 (kg DW m^{-2})	INT	0.58 ± 0.26	0.52	–	–	–	–
	EXT	0.49 ± 0.29	0.47	–	–	–	–
Soil C profile 2006	INT	2.93 ± 0.35	2.98	–	–	0.99	0.13
	EXT	2.74 ± 0.32	2.86	–	–	0.99	0.21
NEE (g C $m^{-2}\ d^{-1}$)	INT	1.06	0.98	2.3(4.1)	2.1(3.8)	0.68	0.13
	EXT	0.66	0.84	1.4(2.5)	1.8(3.2)	0.58	0.11
Harvest (kg DW m^{-2})	INT	0.19	0.19	5.3	5.4	0.54	0.22
	EXT	0.23	0.20	4.8	4.3	0.49	0.26

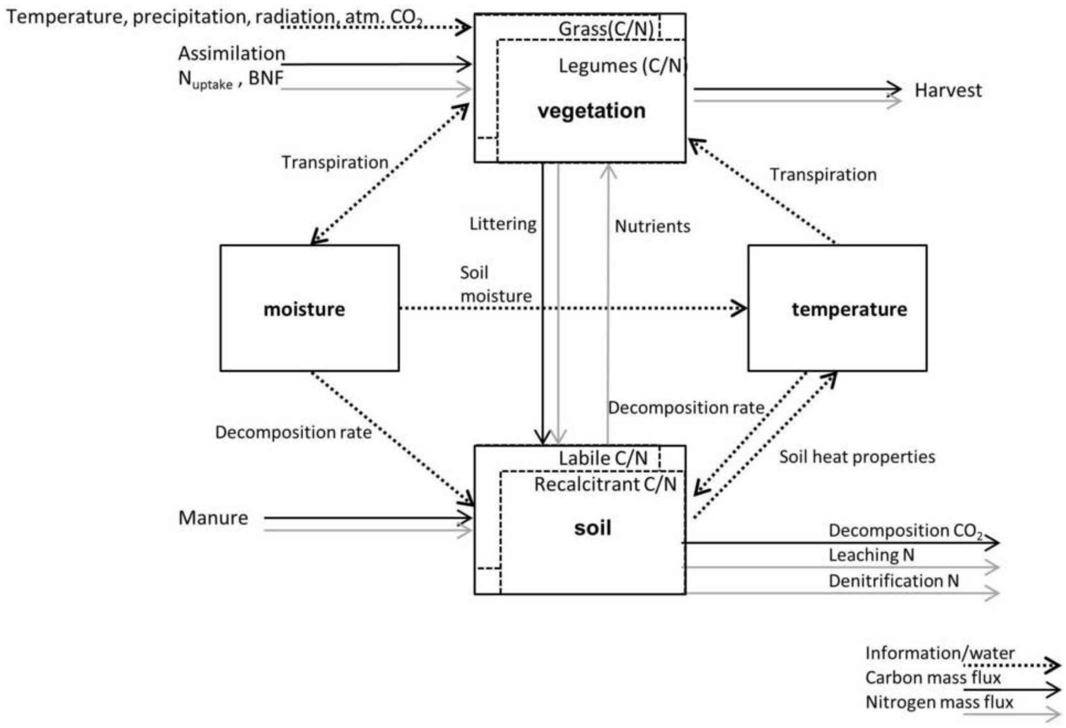

Fig. 1. Overview of the Oensingen Grassland Model. The 4 solid-lined boxes are the main modules. The vegetation module can contain multiple plant functional types (here: grass and legumes in dotted boxes). The soil contains two decomposition pools, expressed in terms of C and N (dotted boxes). Arrows denote relationships between the modules. They can refer either to mass or information fluxes.

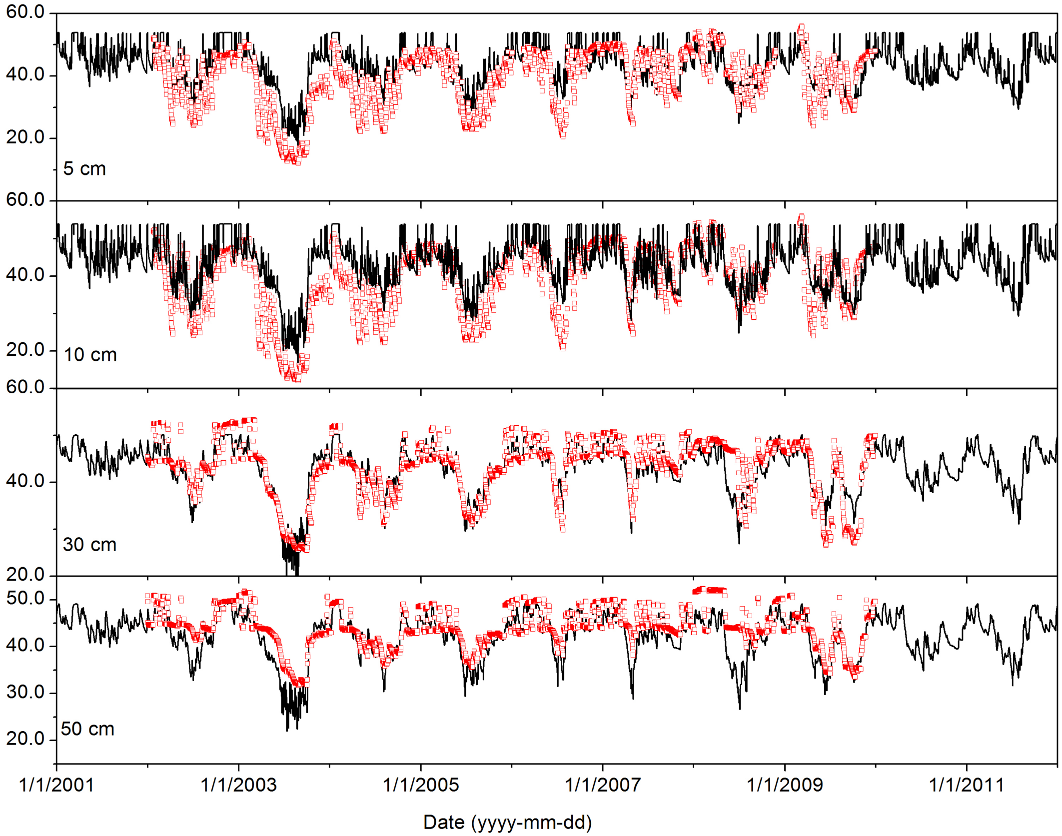

Fig. 2. Soil water content (SWC) expressed in %VOL in increasing soil depth.

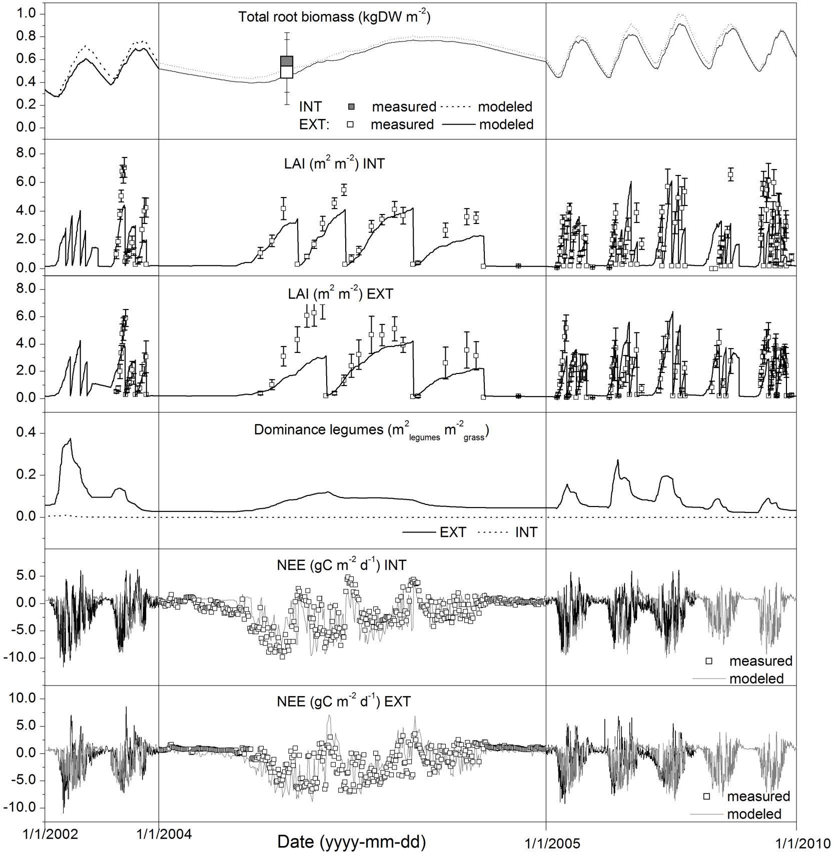

Fig. 3. Simulation results for grassland at Oensingen under extensive management (EXT) and intensive management (INT) in different time scales. Shown are (from top to bottom) sum of modeled root biomass (measured ± se), LAI (measured ± se), modeled foliage surface dominance of legume species, and CO$_2$ exchange. Performance criteria are shown in Table 5.

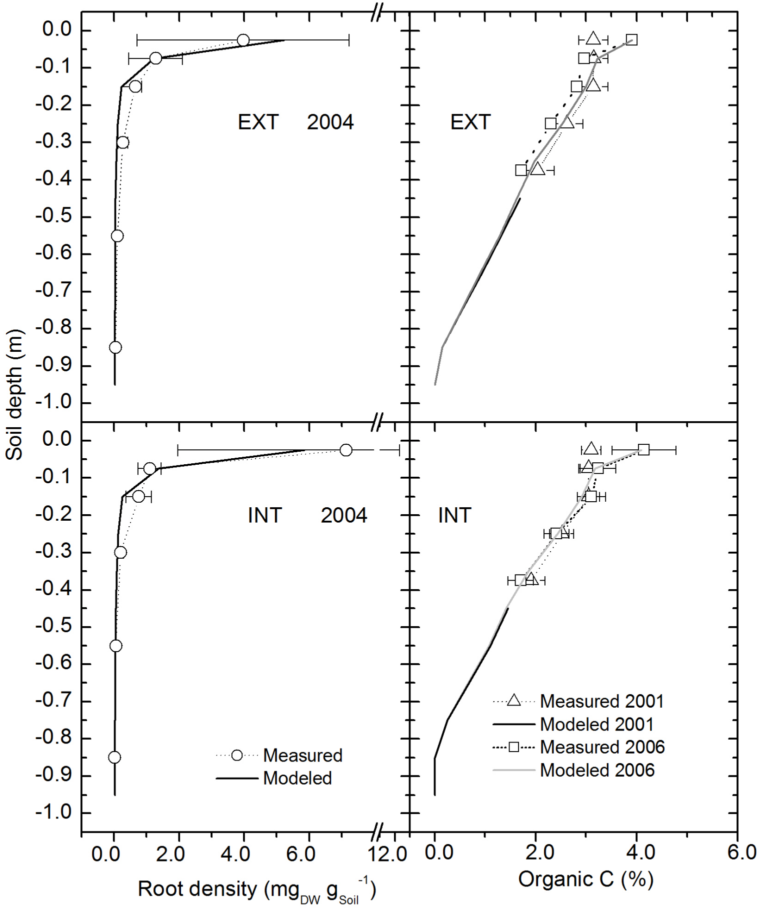

Fig. 4. Root density (left) and soil carbon (right) for EXT (upper pane) and INT (lower pane). Measurements are given ± se.

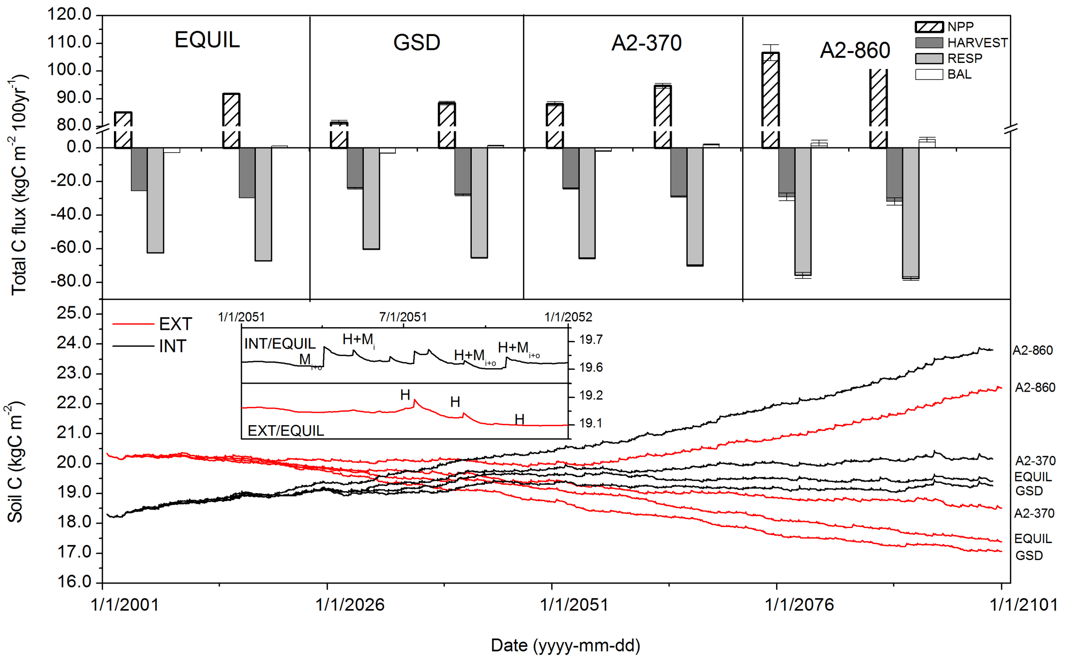

Fig. 5. Simulations of soil organic C (in $\mathrm{g\,C\,m^{-2}}$) between 2001–2100. Top panel: C budget, 100 yr after establishment of grassland. Bottom panel: temporal C dynamics during between 2001–2100 (inset: simulations of SOC between 2051–2052 for INT, upper and EXT, bottom. Management activities are shown as H = harvest; M_i and M_{i+o} = inorganic and organic plus inorganic manure application, respectively). Legend entries: NPP = Net Primary Productivity, Harvest = extracted biomass, Resp: heterotrophic respiration, Bal: C balance (soil+biomass).

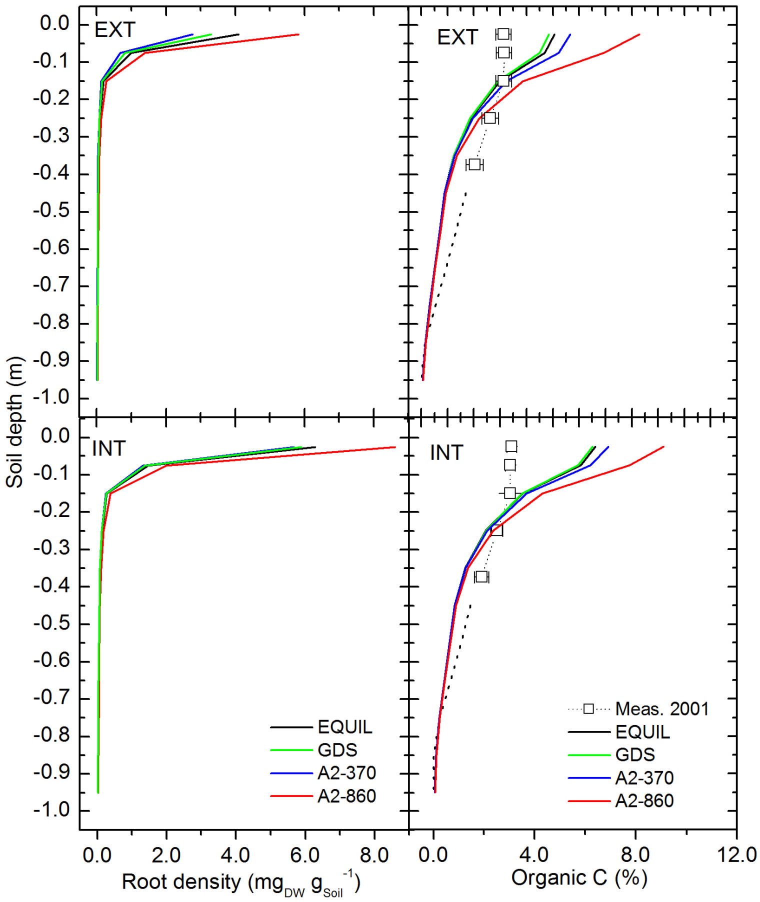

Fig. 6. Simulated root density (left) and soil carbon (right) for EXT (upper pane) and INT (lower pane) in 2001 and 2100 under different climate and management scenarios. Measurements in 2001 are given ±se.